

Multiscale understanding in fracture resistance of bamboo skin

Junhe Cui^{a,b,1}, Mingrui Jiang^a, Marco Nicola^c, Admir Masic^b, Zhao Qin^{a,d,e,*}

^a Department of Civil and Environmental Engineering, Syracuse University, Syracuse, NY 13244, USA

^b Department of Civil and Environmental Engineering, Massachusetts Institute of Technology, Cambridge, MA 02139, USA

^c Department of Chemistry, Università di Torino, Italia

^d Laboratory for Multiscale Material Modeling, Syracuse University, 151L Link Hall, Syracuse University, Syracuse, NY 13244, USA

^e The BioInspired Institute, Syracuse University, NY 13244, USA



ARTICLE INFO

Article history:

Received 14 June 2021

Received in revised form 5 August 2021

Accepted 30 August 2021

Available online 10 September 2021

Keywords:

Bamboo skin

Silica particles

Fracture behavior

Molecular dynamics simulation

Finite element analysis

Material by design

Scanning electron microscopy

ABSTRACT

Bamboo has been widely used in construction for its high strength, lightweight, and low cost. It usually fails from the skin because of macroscopic fiber splitting. Previous research focused on the strength of bamboo at a structural scale without insight into its chemistry and microstructure of the skin and how they relate to its fracture. In this research, we combine multiscale computational modeling with experimental methods to characterize the distribution of silica particles within the bamboo skin and investigate their effect on fracture. We use a microscope to characterize the chemical and microscopic features of bamboo skin and notice silica particles generally distributed in bamboo skin and their pairwise distances follow a normal distribution. We use molecular dynamics simulations and finite element analysis to investigate the effect of silica particles and their unique distribution on the fracture of bamboo skin. It is noted that the silica forms a perfect bonding interface to cellulose fibers and the particles significantly increase the critical stress up to 6.28% than pure cellulose matrix for cracks that randomly occur. We find that such an enhancement in critical stress against random cracks is only guaranteed by the distribution of silica particles in bamboo skin, as such an enhancement is not observed for other randomly assigned silica particles, suggesting that the silica distribution in bamboo skin is optimal for critical stress improvement for random cracks. This research output can inspire the development of more durable and sustainable bamboo products as well as innovative synthetic composite materials.

© 2021 Elsevier Ltd. All rights reserved.

1. Introduction

As the fastest-growing and highest-yielding plant, bamboo is a highly sustainable bio-composite material reinforced with unidirectional strong fibers and silica particles [1–3]. The unidirectional fibers contribute to the remarkable axial mechanics of bamboo (e.g., high unit-weight strength, elastic modulus, and high toughness in tension, etc.), which are comparable with those conventional materials such as fiberglass/steel-reinforced concrete in construction. Chemically treated bamboo fibers can be used as reinforcing agents in thermoplastic polymer matrices [4]. Bamboo has relatively low interlaminar fracture toughness comparing to the strength of the fibers, making it more susceptible to longitudinal fiber splitting failure instead of breaking of fibers in loading. The microscopic cracks on bamboo skin, which initiate

from naturally existing defects (caused by a change of temperature or humidity in growth), can signify crack propagation along fibers at the macroscale. Loading on bamboo structures leads to bending moment perpendicular to the bamboo axis and is responsible for the maximum tensile/compressive stress in the outmost skin, making it easily fracture. Fig. 1a shows the fiber-splitting phenomena accompanying bending and buckling failure. Nevertheless, most previous research on bamboo mechanics focused on macroscale fatigue and fracture behavior of bamboo from the structural level in experiments [5], and we have little idea about crack initiation and its interplay with the chemical and microstructural features on bamboo skin.

We observe a silica-rich layer on the skin of *Pseudosasa amabilis* bamboo, which has been exported from southern China to Italy for the production of tools (e.g., fishing rods, ski poles) where extraordinary flexibility and resistance are required since the 19th century [9]. Analysis of the scanning electron microscopy (SEM) and back-scattered electron (BSE) images (Figs. 1b and 1c) of the bamboo skin reveals that most of the silica is concentrated in the spherical particles. Silica is inducted in the form of silicon from the earth as bamboo cells absorb water [10], and

* Corresponding author at: Department of Civil and Environmental Engineering, Syracuse University, Syracuse, NY 13244, USA.

E-mail address: zqin02@syr.edu (Z. Qin).

¹ Present address: Department of Civil Engineering and Engineering Mechanics, Columbia University, New York City, NY 10027, USA.

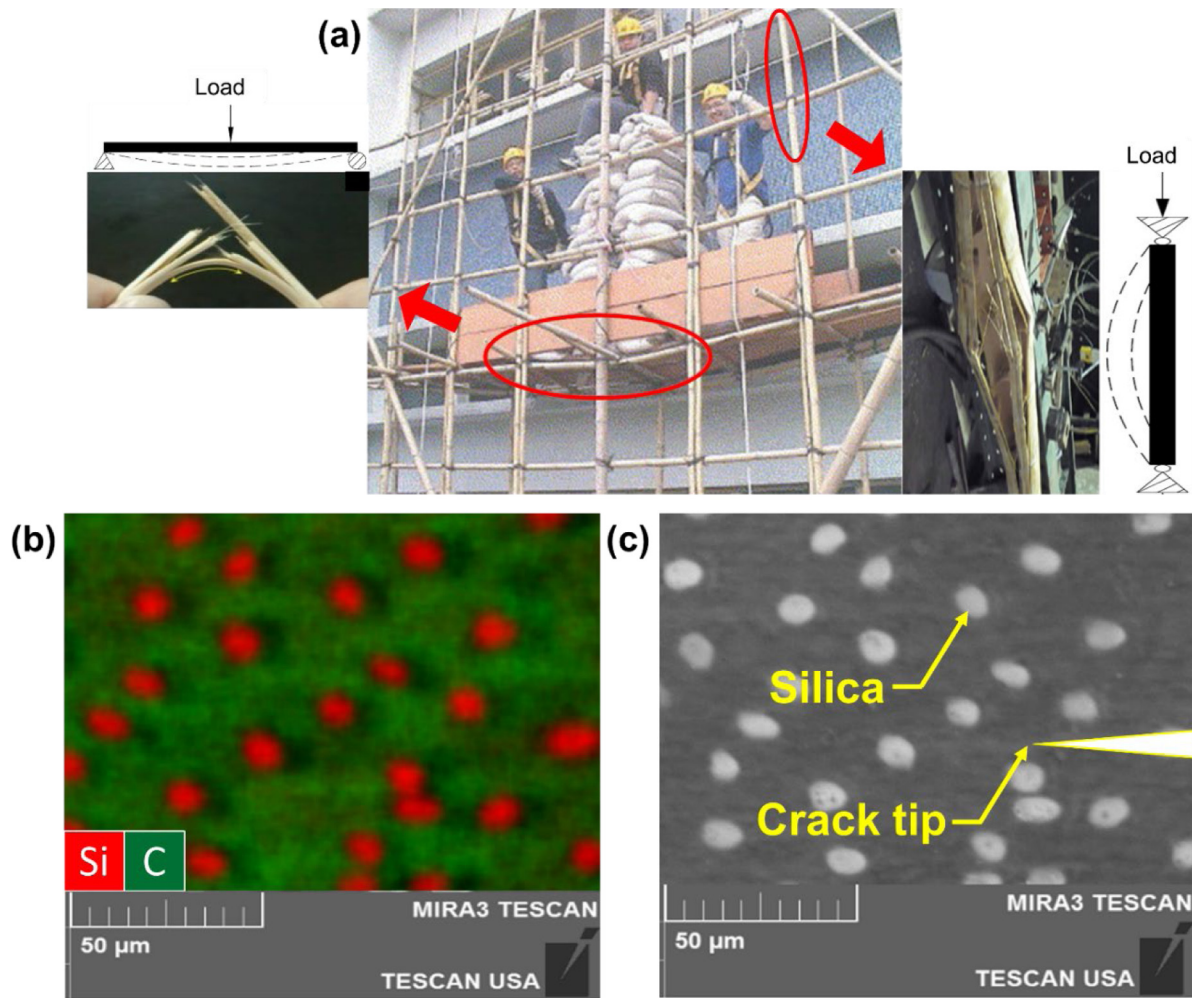


Fig. 1. Structural members made of bamboo and SEM images of bamboo skin. (a) is a typical bamboo scaffolding in a Hong Kong construction site. Reproduced with permission [6]. The fiber splitting phenomena accompanying bending and buckling failure modes of bamboo are shown on the left and right respectively. Reproduced with permission. [7,8] (b) is the BSE image of bamboo skin, on which red and green colors correspond to silica particles and uncovered bamboo skin respectively. (c) is the SEM image showing the distribution of silica particles and a possible crack on bamboo skin.. (For interpretation of the references to color in this figure legend, the reader is referred to the web version of this article.)

is deposited into the epidermis due to silicic acid condensation as a result during transpiration. Former studies investigate the biological functions of silica in bamboo, including accelerating the growth, fortifying the resistance to injury by disease [11], and bio-sequestering carbon in an ambient environment [12]. It is also revealed that phytolith analysis has potential taxonomic significance for identifying bamboo at the genus level [13,14]. Most state-of-the-art studies are focusing on exploiting the potential of biogenic silica from bamboo for novel applications [15], such as synthesizing biocompatible amorphous silica nanoparticles for drug delivery [16] and converting them to nano silicon as an innovative anode material [17]. Previous investigations on mechanical functions of silica in bamboo only disclosed the exceptionally high hardness in the silica cell wall, which would shed light on designing innovative nanocomposite with cell wall polymers reinforced with silica nanoparticles [18]. However, the mechanical function of the silica particles on bamboo has not yet been investigated. The fact that the mineral silica is six times stiffer than the surrounding bamboo matrix makes it interesting to investigate its effect on fracture of bamboo skin [19].

The broad existence of silica particles in bamboo skin turns it into a natural composite material with multiscale features at the interface between two material phases. From the aspect of a continuum, bamboo skin is a composite material with stiff

inclusions (i.e., silica particles) embedded in the relatively soft matrix (i.e., bamboo epidermis). However, at the nanoscale, there is a fine interface between silica and cellulose, the major component of the bamboo epidermis, and the adhesion property of this interface is crucial to the deformation and fracture of bamboo skin at the larger length scales.

In this research, our objectives are to thoroughly investigate the effect of spherical silica particles on crack initiation on bamboo skin, determine the underlying mechanism, and study how this effect varies with the silica distribution pattern. To achieve the research goal, we adopt a bottom-up multiscale modeling strategy. At the nanoscale, we perform molecular dynamics (MD) simulations on atomistic models of silica to bamboo interface and evaluate its adhesion properties to inform the interfacial settings of finite element analysis (FEA) models. At mesoscale, we construct hundreds of FEA models of bamboo skin with silica particles located at different locations relative to the crack tip and measure the critical applied stress (σ_{cr}) to cause the crack to propagate. We also discuss how silica particles affect crack propagation by analyzing SEM images of mechanically cracked samples to justify our computational results. To gain an understanding of the advantage of having silica particles distributed in a certain pattern as observed in bamboo skin (Fig. 1b,c), we thereafter develop our mathematical model to evaluate the effect

of silica particles on fracture enhancement against random cracks and compare the effect with that comes from other randomly distributed silica particles. Our study can help structural engineers design more robust and sustainable structures with bamboo, and inspire material engineers to invent biomimetic composite materials with programmable fracture resistance.

2. Materials and methods

2.1. Scanning electron microscopic (SEM) image of bamboo skin

The *Pseudosasa amabilis* bamboo sample we studied here was a gift to a co-author from the Italian Bamboo Rodmakers Association on October 30, 2016. We analyzed the surface of this bamboo sample under the TESCAN scanning electron microscopy. Our BSE image shows that most of the silica is concentrated within the spherical particles while the rest area of the bamboo skin is uncovered. Our SEM image analysis reveals that the diameter of silica particles is a constant value of 10 μm while the distances between two neighboring silica particles range from 10 μm to 50 μm . The bamboo fibers beneath the silica-rich layer are highly oriented along the same direction (i.e., along the bamboo culm), and there is no fiber deviation or termination around the silica particles. This observation indicates that the bamboo epidermis is a transversely anisotropic material and silica particles adhere to the surface instead of embedding into the fibers. Our multiscale computational models are developed by strictly following the geometric and material information obtained from the experiments.

2.2. Atomistic models of silica to bamboo interface

To understand the interfacial interaction between silica and cellulose at the nanoscale, we build a fully atomistic model of the silica–cellulose interface (Fig. 2a) and use it to study their interaction within the bamboo skin. The cellulose crystal is built by Cellulose-Builder [20] with a dimension of $10 \times 3.2 \times 3.7 \text{ nm}^3$. The silica crystal with the dimension of $14.1 \times 6.8 \times 1.3 \text{ nm}^3$ is built by CHARMM following the procedure and a silica–water force field developed by Lopes et al. [21]. The cellulose crystal is placed on the surface terminated by surface hydroxyl groups, which corresponds to α -quartz (011) surface, which is shown to be the major adsorption site in the solvent [22]. This cellulose–silica model is solvated in a water box of $20.0 \times 8.0 \times 6.4 \text{ nm}^3$, which is large enough to include the model and prevent it from interacting with the mirroring systems. 0.1 M/L NaCl is added to make the system charge neutral. Fig. 3a is the complete atomistic model as captured by VMD [23]. To study the adhesion property at this interface, we perform MD simulation with NAMD package [24] following the boundary conditions as is shown in Fig. 2b: we constraint each atom within the bottom layer of the silica (of 0.4 nm in thickness) by springs of 10 kcal/mol/Å² in all directions and use Steered Molecular Dynamics (SMD) to apply force to the end carbon atoms of the top layer of the cellulose chains by an SMD spring with the stiffness of 20 kcal/mol/Å² and the moving speed of 1 Å/ps. Other key simulation parameters include the 2 ps timestep with rigid bond constraint applied between each hydrogen and the atom to which it is bonded, constant atom number, constant temperature 300 K, constant pressure 1 atm (NPT), full periodic boundary condition in all directions and Particle Mesh Ewald (PME) used for computing electrostatic interactions for periodic boundary conditions.

2.3. Finite element models of bamboo skin

The stiffness of silica is reported to be 72 GPa [25]. The mechanical properties of transversely anisotropic bamboo skin can be described by nine engineering constants (i.e., $E_1 = E_2 = 10.7 \text{ GPa}$, $E_3 = 36.1 \text{ GPa}$, $\nu_{12} = 0.23$, $\nu_{13} = \nu_{23} = 0.1$, $G_{12} = 2.5 \text{ GPa}$, $G_{13} = G_{23} = 8.4 \text{ GPa}$) [26]. We construct a finite element model of bamboo skin (Fig. 3b) with silica particles embedded in the bamboo matrix. A pure bamboo skin model without silica is constructed as a reference. Moreover, we build several types of models with different silica particle layouts (i.e., only the near-tip silica, and all the other silica particles except the near-tip silica) and, in each type of model, we locate the near-tip silica particle at various regions to explore how this effect varies with the relative location of silica particles.

We carry out FEA analysis using ABAQUS version 6.19 to determine critical stress. Our MD simulation indicates that silica particles firmly adhere to bamboo skin. In the FEA models, we simulate this strong adhesion by defining a tie constraint at the contact between silica particles and the bamboo matrix. The dimension of our FEA model is 60 μm by 120 μm , and the crack length is set to 30 μm . An eight-node quadratic plane stress element with reduced integration (CPS8R) is adopted for meshing due to the plane stress nature of this problem. The mesh size of 3 μm is chosen after considering the mesh sensitively by analyzing the mesh sizes ranging from 0.5 to 5 μm . On each model, external stress (σ_r) is applied orthogonally to the crack plane to investigate the mode-I fracture, and the corresponding stress intensity factor (K_I) is computed by FEA. The fracture toughness (K_{IC}) of bamboo skin, which is the critical stress intensity factor for a crack to start propagating, is reported to be $116.2 \text{ MPa}\sqrt{\text{m}}$ [27] in literature. We record the critical applied stress σ_{cr} at which the K_I reaches K_{IC} for further analysis. The contribution of silica particles on the fracture resistance f_R is quantified as the improvement in σ_{cr} in comparing to σ_{cr0} by

$$f_R = \frac{\sigma_{cr}}{\sigma_{cr0}} - 1 \quad (1)$$

where σ_{cr0} is the critical stress for the bamboo skin model without silica particles.

The preliminary results are summarized in Table 1. We notice that the presence of silica particles considerably improves σ_{cr} , and this improvement is highly dependent on the location of silica particles. The results reveal that the critical stress improvement is mainly contributed by the silica particle nearest to the crack tip, while the effect from the silica particles far away from the crack tip is negligible.

Based on these findings, we propose simplified FEA models with only one silica particle whose position of each silica particle is described by the distance from the crack tip (r) and an angle (θ) from the crack propagation (i.e., fiber splitting) direction. This only silica particle is located at many different locations in the crack frontal region, highlighted in Fig. 3c, to investigate how the critical stress improvement varies with the silica particle location relative to the crack tip.

2.4. Bamboo-inspired silica particle distribution and improvement of fracture resistance

The silica distribution pattern on bamboo skin can be quantitatively described as mean (μ_d) and standard deviation (σ_d) of neighboring silica distances. These two parameters are associated with the total number of silica particles within a given area (n) and minimum separation between silica particles (d_{min}). In this research, we need to generate a series of silica distribution patterns with shifted μ_d and σ_d values to make a comparison

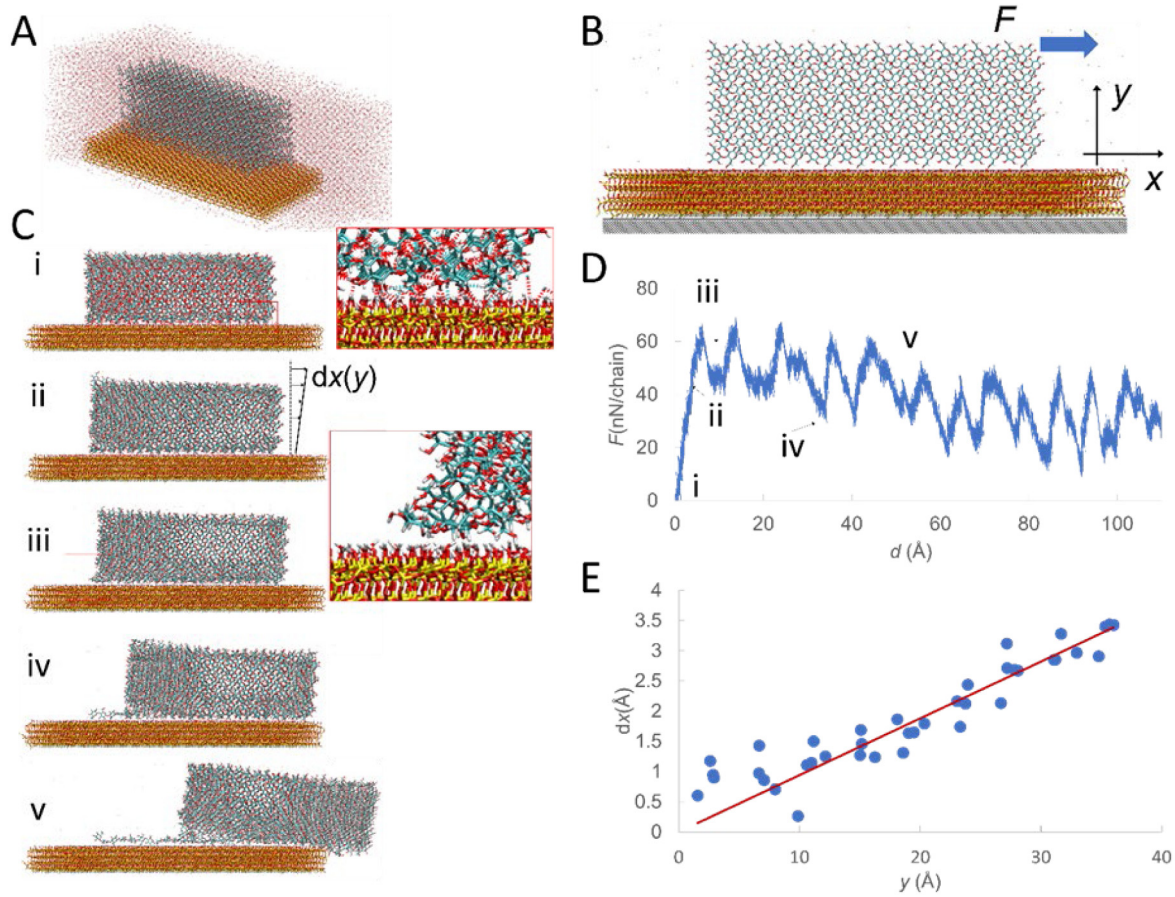


Fig. 2. Atomistic models and MD simulation process. (a) is the atomistic model of silica to cellulose interface. (b) shows the loading configuration. (c) demonstrates different stages in the MD simulation process. (d) is the force–displacement curve during the simulation, and (e) shows the shear strain that is captured during the elastic deformation region (ii in panel C).

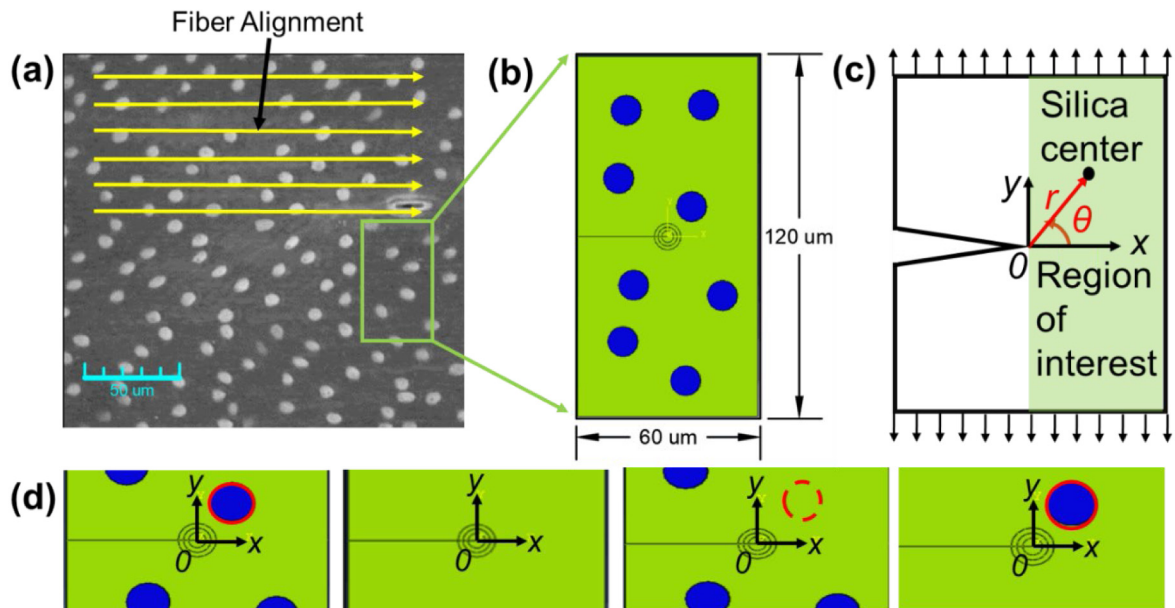




Fig. 3. FEA models of bamboo skin. (a) is the SEM image of bamboo skin, showing silica particles and fiber alignment. (b) shows the initial FEA model with silica particle (blue) attached to a transversely anisotropic bamboo matrix (green). (c) demonstrates the applied loads, coordinate system, and region of interest where near-tip silica particle locates. (d) shows models with different silica arrangements, namely all the silica particles, no silica particle, without near-tip silica particle, and with only near-tip silica particle. The silica particle highlighted in red is moved to different locations in the subsequent simulations.. (For interpretation of the references to color in this figure legend, the reader is referred to the web version of this article.)

Table 1
Summary of improvement in σ_{cr} for near-tip silica at different locations.

Region	Silica center ^a (r, θ)	Improvement in σ_{cr} (%)	
		All the silica particles	Near tip silica particle only
Crack Tip 	(12.8, 51.3)	6.73	6.72
	(11.2, 63.4)	6.62	6.60
	(14.1, 45.0)	6.66	6.63
	(13.5, 21.8)	8.43	8.42
	(14.2, 10.1)	6.09	6.11
	(15.9, 28.2)	4.86	4.96
	(18.0, 33.7)	3.53	3.60
Crack Edge 	(18.0, 146.3)	0.91	0.92
	(14.1, 135.0)	0.64	0.45
	(11.2, 116.6)	0.26	0.27

^aOrigin of the coordinate system is at the crack tip.

with real bamboo skin. To quantify the performance of a specific silica distribution pattern, we perform a series of imaginary tests. Our simulations on the aforementioned simplified FEA generate a scattered dataset consisting of a series of relative silica particle locations to the crack tip, expressed in r and θ , as well as their corresponding critical stress improvement values. For a crack occurring at any location, its propagation direction is always parallel to the bamboo fiber orientation, and its location (r and θ) is with respect to the nearest silica particle. The critical stress improvement for a crack initiated at any location is approximated by the natural neighbor interpolation method [28]. The critical stress improvement values are computed for 100, 200, 500, 1000, and 2000 random locations on bamboo skin to get a convergent result.

3. Results

3.1. Atomic adhesion between silica to the bamboo epidermis

The MD simulation trajectory is shown in Fig. 2c. From this trajectory, we notice as the cellulose chains are pulled along the silica substrate, the cellulose block deforms but the chain closest to the silica substrate remains attached to the silica substrate. Fig. 2d shows the full force–displacement curve of the cellulose as recorded during the simulation, with the force normalized by the number of chains being pulled. It is shown the peak force at the end of the elastic region (iii of Fig. 2c) is recorded as 65 nN/chain, leading to the shear strength of 10 GPa that is significantly higher than the yield strength of silica or wood matrix [29,30], suggesting that the silica and cellulose form an ideal interface without relative sliding until failure taken place in one of the material phases in an extreme loading condition. Fig. 2e shows the horizontal displacement of cellulose chains at different vertical locations relative to the surface of the silica substrate. The linear trend with a horizontal transect close to zero further proves that the cellulose chain keeps connected to the substrate, coinciding with what is shown on the trajectory. The Hydrogen bonds formed between cellulose and silica contribute to the strong adhesion of this interface. The simulation results indicate that the silica particles can be reasonable assumed to be tied to the bamboo epidermis.

3.2. Critical stress improvement attributed by near-tip silica particle

The surface plot (Fig. 4a) reveals that critical stress improvement highly depends on both r and θ . Generally speaking, a higher improvement can be achieved if the silica particle is placed closer to the crack tip or the angle formed between the silica center and crack tip is smaller. For a silica particle with a given r , the highest improvement will be achieved if θ is 0° . The improvement

gradually drops as the angle θ increases until the lowest value is reached when θ is 90° . In contrast, the minimum improvement value is constant at a negligible value. This information justifies that it is reasonable to study silica particles at the crack frontal area.

We studied the stress distribution pattern around the crack tip for models with silica at different regions under the same external loads. On the pure skin model (Fig. 4c), we notice symmetric stress distribution and a high-stress concentration at the crack tip. The crack starts to propagate once this concentrated stress reaches the yield strength of bamboo skin [31,32]. To the contrast, we observe an unsymmetric stress distribution and a significant reduction in the stress concentration at the crack tip on the other two models (Fig. 4d and 4e), indicating that a higher external load is expected to be resisted by these models. We notice, instead of following the straight fiber orientation, cracks deflect near silica particles (Fig. 4f). These findings reveal that the mechanisms for silica particles to enhance fracture resistance are stress delocalization and crack deflection. The crack deflection phenomenon also proves that the impact of silica particles on the fracture behavior of bamboo skin is significant.

3.3. Silica distribution pattern on bamboo skin

Actually, instead of having any pre-existing crack [33], cracks in bamboo skin can randomly initiate at any location on bamboo skin, and the least improvement will be achieved when a crack happens right in the middle of two silica particles, where distance r is maximized. Hence, the overall fracture performance of bamboo skin is governed by neighboring silica distances. We measure and plot the probability density of the distances (d_{ij}) from a silica to its near neighbors (contribute to the first peak of the radial distribution function of the silica particles) based on the SEM image of our bamboo sample (Fig. 5a). We notice that this distribution follows a normal distribution pattern, with a mean value (μ_d) of 27 μm and standard deviation (σ_d) of 7.8 μm . The total number of silica particles is counted to be 148 within an area of 300 μm by 300 μm .

3.4. Statistical analysis on improvement in fracture resistance

A series of imaginary tests are performed to quantify the contribution of silica particles on the fracture resistance (Fig. 5b). The results reveal that 1000 fracture tests are enough to produce convergent results. We find the silica particles on bamboo skin contribute to a mean (\bar{f}_R) of 6.28% increase in fracture resistance. A silica distribution layout can be quantitatively described by three parameters, namely average neighboring silica distance (μ_d), non-uniformity (σ_d), and total particle numbers (N). To explore how the critical stress improvement is affected by each

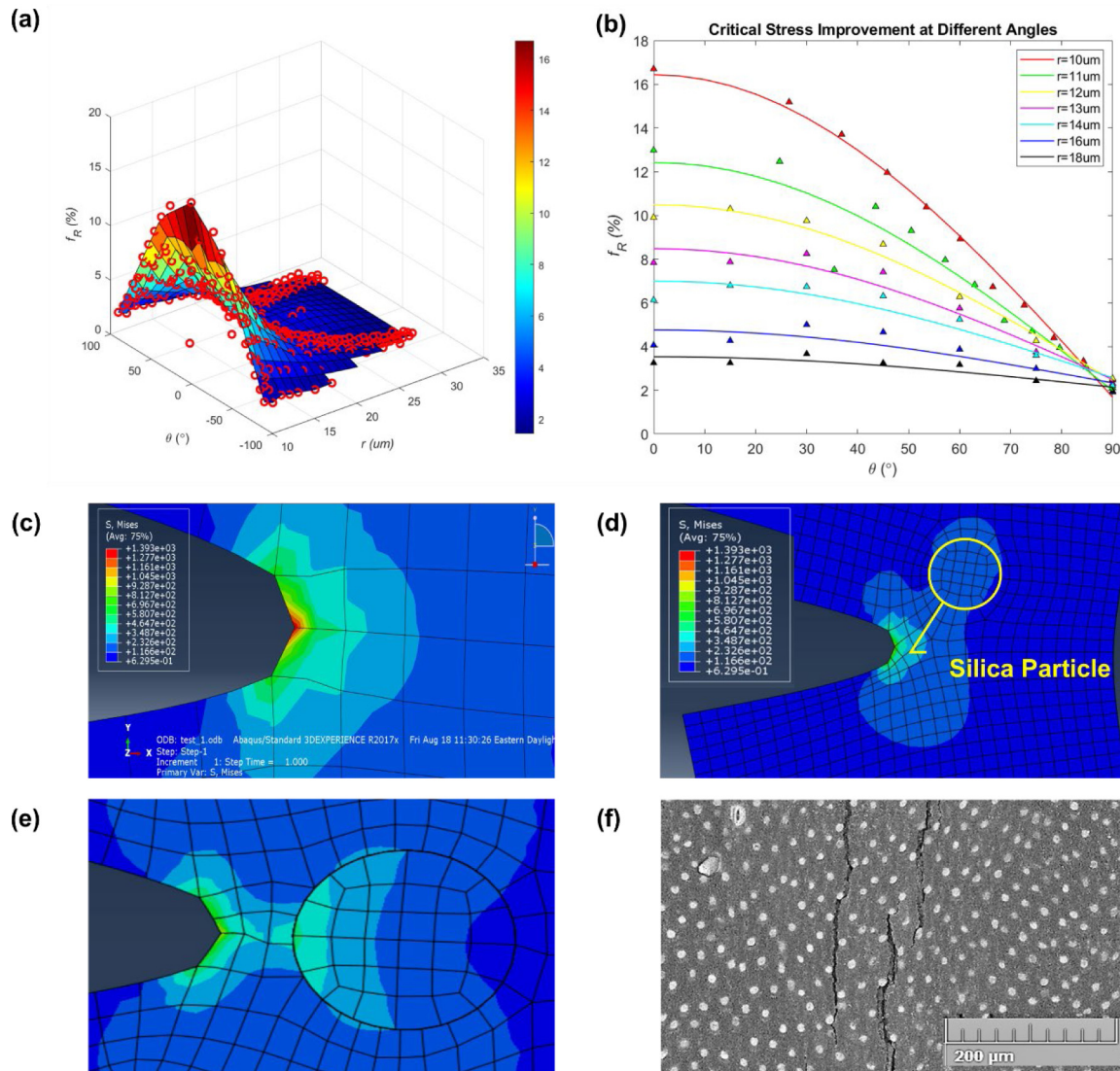


Fig. 4. Effect of silica particles on critical stress improvement. (a) is the surface plot showing the percentage of critical stress improvement due to the presence of a single silica particle located at each specific location. The results are reorganized by r (b). (c–e) corresponds to stress (σ_{11}) distribution near the crack tip for bamboo skin models with no silica, silica at 45° , and silica right in front of the crack tip. (f) is the SEM image shows crack deflection near silica particles.

of these parameters respectively, we perform imaginary tests on several designed silica groups (Fig. 5c) At least one of the parameters of each group is kept the same with another group in order to evaluate the impact of each parameter. Both larger or smaller values of each parameter are chosen to explore whether the silica layout on bamboo is optimal for mechanical strength. The results are summarized in Fig. 5d, and generally, the overall improvement depends on both the μ_d and σ_d . Group A has the same μ_d with bamboo while σ_d is increased to 12.9 μm . Its computed \bar{f}_R is 20% smaller than that of bamboo. If μ_d rises to 32 μm (Group B), the μ_i will be further decreased to about 74% of that of bamboo. The μ_d in Group C is shifted to 23 μm but the σ_d is kept as the same as bamboo. Though much more silica particles are fitted in the same area, the performance of this layout in resisting cracks is almost the same as that of bamboo. If σ_d is increased to 11.5 μm (Group D), the same number of silica particles with bamboo will be placed, but the μ_i contributed by this layout is only about 80% of that by bamboo skin. There are numerous other possible layouts for 148 particles. Group E ($\mu_d = 24 \mu\text{m}$, $\sigma_d = 6.7 \mu\text{m}$) is an example, and this layout can produce a comparable improvement with bamboo. As expected, if the σ_d

is increased to 9.1 μm (Group F), the improvement will drop by 10%.

Based on these results, we can see that the critical stress improvement largely depends on the silica distribution pattern rather than the number of silica particles alone. The $1/\mu_d^2$ value is proportional to the average number of silica particles within the given area, while σ_d defines the nonuniformity of the distribution. In general, the \bar{f}_R value keeps decreasing as the μ_d value of silica distribution becomes greater which corresponds to the case when the particles separate further from their neighbors. Moreover, for a given μ_d , the \bar{f}_R value reduces as the neighboring particle distances become more non-uniform (i.e., a larger σ_d). Overall speaking, silica particle distribution on bamboo is optimal for enhancing fracture resistance based on the comparisons with other representative cases.

4. Discussions

The embedment of stiff inclusion in a soft matrix is a promising means for designing engineering composite materials [34,35]. Nevertheless, how the mechanical performances of the composite materials are affected by the addition of such stiff inclusions

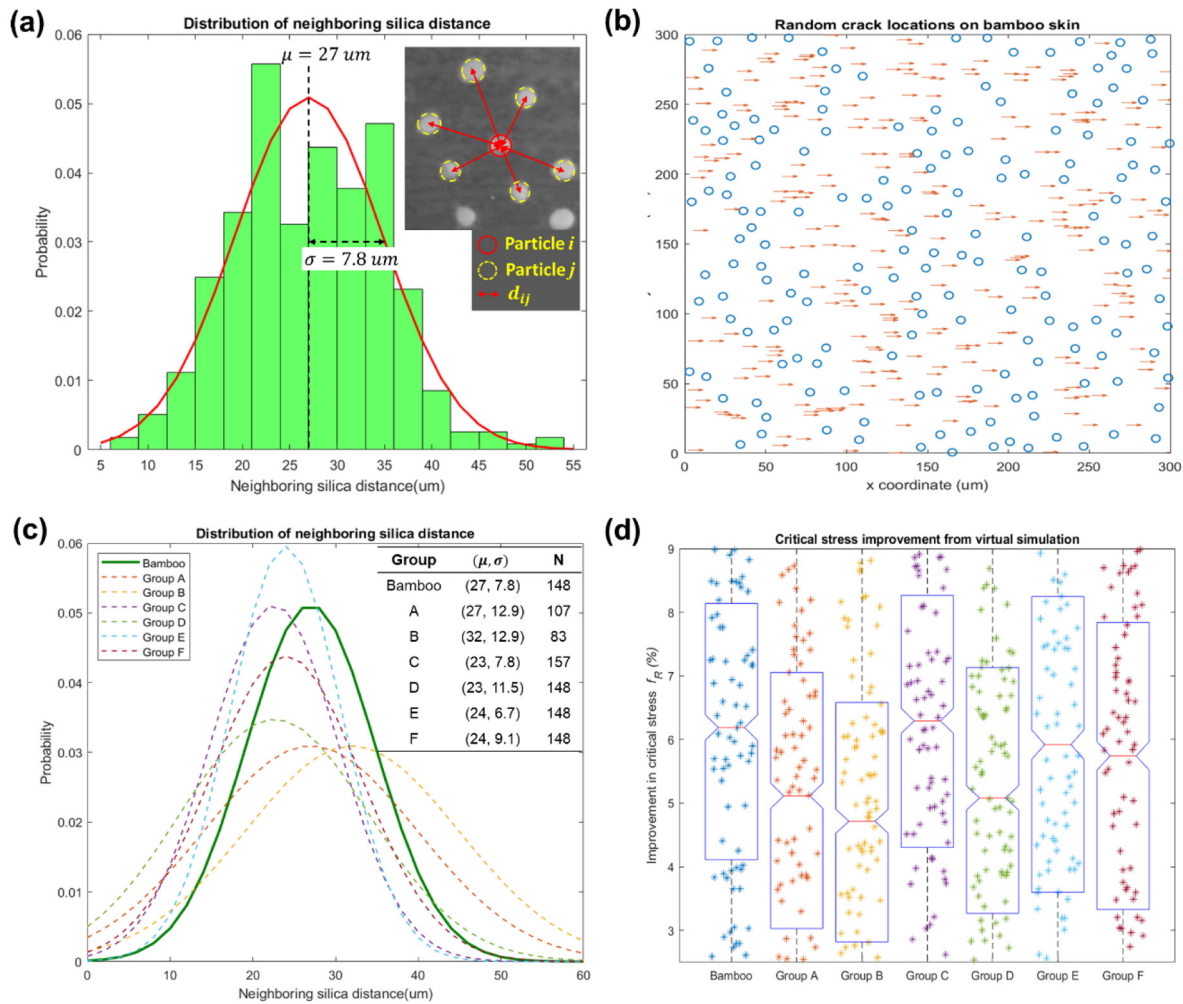


Fig. 5. Silica distribution pattern and critical stress improvement. (a) illustrates the measurement of neighboring silica distances of particle i , and plots the probability density function of the measured results. (b) shows the randomly initiated cracks on bamboo skin for our imaginary tests. (c) shows groups of designed silica distribution patterns with shifted μ_d and σ_d , and the statistical analysis of the results of the imaginary tests are plotted in (d).

remains unclear, and material scientists have little idea on engineering the composite properties by manipulating the inclusions. Our research output will shed light on addressing these challenges. We may inspire the design of biomimetic composite materials with enhanced fracture resistance by inserting stiff inclusions following bamboo’s skin. However, this research concentrates on the silica particles on real bamboo skin, where only the near-tip one contributes to fracture resistance because others are too far away to be effective. It is also meaningful to study how the fracture resistance is affected when multiple silica particles locate within effective range. Actually, the stress intensity factor at the crack tip largely depends on the model geometry, and here our computational model is constructed just to demonstrate the concept. A quantitative study of the size or scaling effect can be done with the FEA and statistical models, as well as 3D printing as following-up studies. Future studies that specifically focus on composite material design may systematically investigate these mechanical enhancements from patterned inclusions.

The superiority of bamboo with silica particles motivates us to manipulate the mechanical properties of bamboo from a chemical perspective. Future researchers may concentrate on understanding the silicification process from an atomistic scale upwards. Once we figure out how environmental factors affect the deposition of silica on bamboo skin, we may be inspired to produce bamboo with our desired properties by smartly selecting the

agriculture strategies, thereby enabling us to make better usage of bamboo. Structural engineers can design more robust and reusable scaffoldings with the engineered bamboo. Moreover, this breakthrough will make it possible to replace traditional construction materials with engineered bamboo on more occasions to enhance the sustainability and cost-efficiency of the built environment.

5. Conclusions

In this research, we observe a silica-rich layer on the skin of *Pseudosasa amabilis* bamboo, and most of the silica is concentrated in spherical particles. Our MD simulation results reveal that silica particles firmly adhere to bamboo fibers through hydrogen bonds and non-bonded interactions at the cellulose–silica interface before the failure of cellulose fibers in shearing. Our FEA analysis results show that the presence of silica particles significantly improves the fracture resistance of bamboo skin. The improvement highly depends on the relative position of the silica particles. A silica particle gives a more significant improvement if it locates closer to the crack tip or the angle formed between the silica center and crack tip is smaller.

Due to nature that a crack can randomly take place, the overall fracture resistance of bamboo skin depends on the distribution of neighboring silica particle distances instead of the relative

position to a pre-existing crack. Our statistical analysis shows that the separation between neighboring silica particles follows a normal distribution pattern ($\mu_d = 27 \text{ um}$, $\sigma_d = 7.8 \text{ um}$). As is computed by our imaginary simulations, for cracks that occur at any location of bamboo skin, the mean improvement in critical stress by comparing to the skin without silica particles (\bar{f}_R) is 6.28%. We notice the improvement value highly depends on the silica distribution pattern, and the real silica distribution pattern on bamboo is proved to be optimal by comparing with the improvement produced by many other distribution patterns.

Our research output will inspire material scientists to design synthetic composite materials by inserting stiff inclusions into the flexible matrix material and manipulating their fracture resistance by setting the distribution of the stiff inclusions [36]. Instead of looking for an optimized pattern with a pre-existing crack, the current study may provide a more comprehensive consideration of composite design, as a crack can randomly take place within the matrix material. Here we use the simple normal distribution to describe the location of the silica particles but by considering more complex particle distribution functions at a larger scale, we may further optimize the fracture resistance of the composite. Such a further study can be done by learning from massive high throughput data and advanced statistical methods including machine learning. The results can be further validated by multi-material 3D printing and mechanical tests. With such a deeper understanding of the mechanical properties of bamboo in mind, structural engineers will be motivated to use bamboo as a structural material as much as possible so that a more sustainable built environment will be achieved. In the future, it is intriguing to figure out how the silica distribution pattern in bamboo is affected by the environment and explore the possibility of engineering the properties of bamboo by adjusting the growing conditions.

Declaration of competing interest

The authors declare that they have no known competing financial interests or personal relationships that could have appeared to influence the work reported in this paper.

Acknowledgments

MJ acknowledges the University Fellowship at SU for supporting the research work. The authors acknowledge Hyun-Chae Chad Loh for helping with the setup and taking SEM image of the cracked sample.

References

- [1] M.K. Habibi, Y. Lu, Crack propagation in bamboo's hierarchical cellular structure, *Sci. Rep.* 4 (1) (2014) 1–7.
- [2] Z.-P. Shao, C.-H. Fang, G.-L. Tian, Mode I interlaminar fracture property of moso bamboo (*Phyllostachys pubescens*), *Wood Sci. Technol.* 43 (5–6) (2009) 527–536.
- [3] P. Van der Lugt, A. Van den Dobbelsteen, J. Janssen, An environmental economic and practical assessment of bamboo as a building material for supporting structures, *Constr. Build. Mater.* 20 (9) (2006) 648–656.
- [4] E. Yuanita, Ismojo, H. Adi, M. Chalid, Crystallinity index evaluation of *Dendrocalamus asper* fibers through variation of chemical treatment, *AIP Conf. Proc.* 2175 (1) (2019) 020060, AIP Publishing LLC.
- [5] E.O. Onche, O.K. Oyewole, J.D. Obayemi, N.B. Ekwe, N. Rahbar, W.O.J.C.E. Soboyejo, Fracture and fatigue behavior of *Bambusa Vulgaris-Schrad* Bamboo, 8, (1) 2021, 1914289.
- [6] W. Yu, K.F. Chung, S.L. Chan, Axial buckling of bamboo columns in bamboo scaffolds, *Eng. Struct.* 27 (1) (2005) 61–73.
- [7] S.-T. Tsai, L.-M. Wang, Huang, Z. Yang, C.-D. Chang, T.-M. Hong, Acoustic emission from breaking a bamboo chopstick, *Phys. Rev. Lett.* 116 (3) (2016) 035501.
- [8] M. He, Z. Li, Y. Sun, R. Ma, Experimental investigations on mechanical properties and column buckling behavior of structural bamboo, *Struct. Des. Tall Special Build.* 24 (7) (2015) 491–503.
- [9] L. Cheng, S. Adhikari, Z. Wang, Y. Ding, Dynamic variation of fuel properties of tonkin cane (*Pseudosasa amabilis*) during maturation, *Energy Fuels* 29 (4) (2015) 2408–2415.
- [10] S. Li, Q. Liu, B. Zhou, G.R.O.O.T. K. de, Calcium phosphate formation induced on silica in bamboo, *J. Mater. Sci. Mater. Med.* 8 (7) (1997) 427–433.
- [11] H. Ueda, Resistivity striations in germanium single crystals, *J. Phys. Soc. Japan* 16 (1) (1961) 61–66.
- [12] S. Li, Q. Liu, J. De Wijn, K. De Groot, B. Zhou, Biomimetic coating of bioactive ceramic on bamboo for biomedical applications, *J. Mater. Sci. Lett.* 15 (21) (1996) 1882–1885.
- [13] X. Tao others, Phytolith sizes and assemblages differentiate genera and ecotypes of woody bamboos in subtropical southwest China, 272, 2020, 104129.
- [14] M.A. Nawaz others, Phytolith formation in plants: from soil to cell, 8, (8) 2019, p. 249.
- [15] N. Sapawe, N.S. Osman, M.Z. Zakaria, Sasm Fikry, Mamjmt Aris, Synthesis of green silica from agricultural waste by sol-gel method, 5, (10) 2018, pp. 21861–21866.
- [16] S. Rangaraj, R.J.A.N Venkatachalam, A lucrative chemical processing of bamboo leaf biomass to synthesize biocompatible amorphous silica nanoparticles of biomedical importance, 7, (5) 2017, pp. 145–153.
- [17] S. Silviana, W.J. Bayu, Silicon conversion from bamboo leaf silica by magnesiothermic reduction for development of li-ion battery anode, in: *Matec Web of Conferences*, Vol. 156, EDP Sciences, 2018, p. 05021.
- [18] Z. Yu, Z. Jiang, X. Zhang, Y.J.W. Yu, F. Science, Mechanical properties of silica cells in bamboo measured using in-situ imaging nanaindentation, 48, (4) 2016, pp. 228–233.
- [19] A.A. Griffith, VI, The phenomena of rupture and flow in solids, *J. Philos. Trans. Royal Soc. London. Ser. A Contain. Pap. Math. Phys. Charac.* 221 (582–593) (1921) 163–198.
- [20] T.C.F. Gomes, M.S. Skaf, Cellulose-builder: A toolkit for building crystalline structures of cellulose, 33, (14) 2012, pp. 1338–1346.
- [21] E. Lopes, V. Murashov, M. Tazi, E. Demchuk, A.D. MacKerell, Development of an empirical force field for silica. Application to the quartz- water interface, *J. Phys. Chem. B* 110 (6) (2006) 2782–2792.
- [22] M.L. Hair, Hydroxyl groups on silica surface, *J. Non-Cryst. Solids* 19 (1975) 299–309.
- [23] W. Humphrey, A. Dalke, K. Schulten, VMD: visual molecular dynamics, *J. Mol. Graph.* 14 (1) (1996) 33–38.
- [24] J.C. Phillips others, Scalable molecular dynamics on CPU and GPU architectures with NAMD, *J. Chem. Phys.* 153 (4) (2020) 044130.
- [25] E.C. Silva, L. Tong, S. Yip, K.J. Van Vliet, Size effects on the stiffness of silica nanowires, *Small* 2 (2) (2006) 239–243.
- [26] J. Cui, Z. Qin, A. Masic, M.J. Buehler, Multiscale structural insights of load bearing bamboo: A computational modeling approach, *J. Mech. Behav. Biomed. Mater.* (2020) 103743.
- [27] S. Amada, S. Untao, Fracture properties of bamboo, *Composites B* 32 (5) (2001) 451–459.
- [28] Q. Zhu, J. Feng, J. Huang, Natural neighbor: A self-adaptive neighborhood method without parameter K, *Pattern Recognit. Lett.* 80 (2016) 30–36.
- [29] S.C. Chowdhury, B.Z.G. Haque, J.W. Gillespie, Molecular dynamics simulations of the structure and mechanical properties of silica glass using ReaxFF, *J. Mater. Sci.* 51 (22) (2016) 10139–10159.
- [30] J.E. Winandy, R.M. Rowell, *The Chemistry of Wood Strength*, ACS Publications, 1984.
- [31] O. Allix, A. Corigliano, Modeling and simulation of crack propagation in mixed-modes interlaminar fracture specimens, *Int. J. Fract.* 77 (2) (1996) 111–140.
- [32] D. Hasselman, Unified theory of thermal shock fracture initiation and crack propagation in brittle ceramics, *J. Am. Ceram. Soc.* 52 (11) (1969) 600–604.
- [33] M.G. Hall, G.E. Lloyd, The SEM examination of geological samples with a semiconductor back-scattered electron detector, *Am. Mineral.* 66 (3–4) (1981) 362–368.
- [34] G. Falzone others, The influences of soft and stiff inclusions on the mechanical properties of cementitious composites, *Cement Concr. Compos.* 71 (2016) 153–165.
- [35] A. Yu, Modeling mechanical behaviors of composites with various ratios of matrix-inclusion properties using movable cellular automaton method, *Def. Technol.* (1) (2015) 18–34.
- [36] G.X. Gu, C.-T. Chen, Mijeml Buehler, De novo composite design based on machine learning algorithm, 18, 2018, pp. 19–28.